Photochemical & Photobiological Sciences

Accepted Manuscript

This is an *Accepted Manuscript*, which has been through the Royal Society of Chemistry peer review process and has been accepted for publication.

Accepted Manuscripts are published online shortly after acceptance, before technical editing, formatting and proof reading. Using this free service, authors can make their results available to the community, in citable form, before we publish the edited article. We will replace this *Accepted Manuscript* with the edited and formatted *Advance Article* as soon as it is available.

You can find more information about *Accepted Manuscripts* in the Information for Authors.

Please note that technical editing may introduce minor changes to the text and/or graphics, which may alter content. The journal's standard Terms & Conditions and the Ethical guidelines still apply. In no event shall the Royal Society of Chemistry be held responsible for any errors or omissions in this *Accepted Manuscript* or any consequences arising from the use of any information it contains.

ROYAL SOCIETY OF CHEMISTRY

www.rsc.org/pps

Photoconversion changes bilin chromophore conjugation and protein secondary structure in the violet/orange cyanobacteriochrome NpF2163g3

Sunghyuk Lim[1], Nathan C. Rockwell[2], Shelley S. Martin[2], Jerry L. Dallas[1], J. Clark Lagarias[2], and James B. Ames[1]*

[1]Departments of Chemistry and [2]Molecular and Cellular Biology, University of California, Davis, CA 95616.

*To whom correspondence should be addressed: E-mail: jbames@ucdavis.edu.

Key words: photoreceptor, CBCR, phytochrome, cyanobacteria, tetrapyrrole, NMR.

Abstract Cyanobacteriochromes (CBCRs) are cyanobacterial photoreceptors distantly related to phytochromes. All CBCRs examined to date utilize a conserved Cys residue to form a covalent thioether linkage to the bilin chromophore. In the insert-Cys CBCR subfamily, a second conserved Cys can covalently link to the bilin C10 methine bridge, allowing detection of near-UV to blue light. The best understood insert-Cys CBCR is the violet/orange CBCR NpF2164g3 from *Nostoc punctiforme*, which has a stable second linkage in the violet-absorbing dark state. Photoconversion of NpF2164g3 leads to elimination of the second linkage and formation of an orange-absorbing photoproduct. We recently reported NMR chemical shift assignments for the orange-absorbing photoproduct state of NpF2164g3. We here present equivalent information for its violet-absorbing dark state. In both photostates, NpF2164g3 is monomeric in solution and regions containing the two conserved Cys residues essential for photoconversion are structurally disordered. In contrast to blue light receptors such as phototropin, NpF2164g3 is less structurally ordered in the dark state than in the photoproduct. The insert-Cys insertion loop and C-terminal helix exhibit light-dependent structural changes. Moreover, a motif containing an Asp residue also found in other CBCRs and in phytochromes adopts a random-coil structure in the dark state but a stable α-helix structure in the photoproduct. NMR analysis of the chromophore is consistent with a less ordered dark state, with A-ring resonances only resolved in the photoproduct. The C10 atom of the bilin chromophore exhibits a drastic change in chemical shift upon photoconversion, changing from 34.5 ppm (methylene) in the dark state to 115 ppm (methine) in the light-activated state. Our results provide structural insight into the two-Cys photocycle of NpF2164g3 and the structurally diverse mechanisms used for light perception by the larger phytochrome superfamily.

Graphical abstract

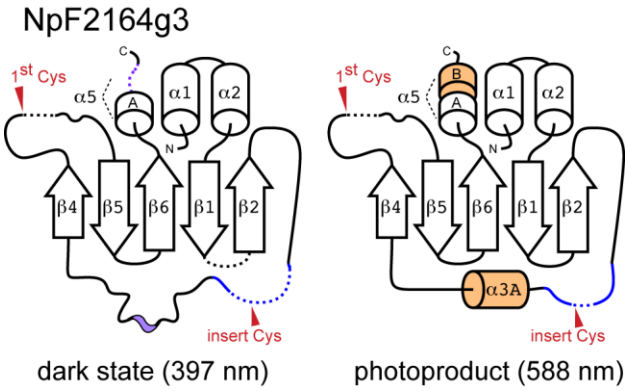

We report secondary structure assignments for the cyanobacteriochrome NpF2164g3 in the violet-absorbing dark-adapted state. Comparison with our previous work on the orange-absorbing photoproduct elucidates structural changes occurring upon photoconversion.

Introduction

Phytochromes are photosensory proteins utilizing covalently attached linear tetrapyrrole (bilin) chromophores. In cyanobacterial phytochromes such as Cph1,[1] the incorporated bilin is phycocyanobilin (PCB), which is covalently attached to a conserved Cys residue at the N-terminal end of a conserved α-helix in a bilin-binding GAF domain.[2-8] The phytochrome superfamily also includes distantly related cyanobacterial photoreceptors called cyanobacteriochromes (CBCRs).[9-11] There are several known CBCR subfamilies.[9, 12] In both phytochromes and CBCRs, light absorption triggers photoisomerization about the 15,16-bilin double bond via a conical intersection.[10-25] Primary photoisomerization of the dark-adapted state is followed by a series of reactions on the electronic ground-state surface to generate a photoproduct state which can either revert to the dark state thermally or via light absorption.[1, 20, 26-29] Thus, phytochromes and CBCRs typically adopt two stable photostates with spectrally and biochemically distinct properties. The dark-stable state most frequently harbors a *15Z* bilin chromophore, which is the product of the bilin biosynthesis pathway in the cell.[30] Canonical phytochromes have red-absorbing *15Z* dark states and far-red-absorbing *15E* photoproduct states,[11] whereas CBCRs have more spectrally diverse photocycles.[9, 12, 19, 20, 31, 32]

The recent determination of crystal structures for red/green and DXCF CBCRs[21, 23] confirmed that these CBCR subfamilies share a bilin-binding GAF fold similar to that of phytochrome (Fig. 1A). Both CBCR subfamilies retain the Cys residue found in Cph1 and the helix on which it resides. In DXCF CBCRs, a second conserved Cys forms a covalent linkage to the bilin to allow detection of violet or blue light.[12, 15, 21, 23, 33-35] Such two-Cys photocycles have independently evolved multiple times.[12] Like DXCF CBCRs, the insert-Cys CBCR subfamily exhibits two-Cys photocycles; however, insert-Cys CBCRs use a structurally distinct second Cys residue.[12] In DXCF CBCRs, the second Cys is part of an Asp-Xaa-Cys-Phe motif that also includes a much more broadly conserved Asp residue.[19, 32, 33] The DXCF CBCRs are thus defined by the presence of a Cys residue in this Asp-motif. In contrast, insert-Cys CBCRs have an Asp-motif closely related to that found in red/green CBCRs,[20] and the second Cys is located in a large,

variable insertion loop.[12] There is currently no structural information available for insert-Cys CBCRs at atomic resolution.

Here, we focus on NpF2164g3 as a model system for structure/function studies on insert-Cys CBCRs. NpF2164g3 is one of several CBCR domains arranged in tandem in a putative phototaxis protein encoded by the *NpF2164* locus in *Nostoc punctiforme*.[12, 20] In NpF2164g3, the two conserved Cys residues are Cys546 and Cys591 and the two photostates are a violet-absorbing *15Z* dark state and a *15E* orange-absorbing photoproduct.[12] Cys591 is broadly conserved in CBCRs and phytochromes and is covalently attached to the chromophore in both photostates (Fig. 2). The insert Cys (Cys546) has been shown to be attached to the bilin C10 atom in the NpF2164g3 dark state by site-directed mutagenesis and biochemical studies including cleavage with hydrogen peroxide,[12] as summarized in Fig. 2. Photoconversion leads to elimination of the thioether linkage at C10, lengthening the bilin conjugated system. This produces the large red shift of the chromophore in the *15E* photoproduct state and permits reaction of Cys546 with iodoacetamide (IAM), which prevents regeneration of the violet state.[12] Biological signaling is thought to arise via propagation of structural changes to adjacent domains, but atomic resolution structures of NpF2164g3 in both states are needed to elucidate such changes. As a first step toward this goal, we recently reported backbone chemical shifts and secondary structure assignments for the orange-absorbing photoproduct state of NpF2164g3.[36] We now report detailed NMR resonance assignments for its violet-absorbing dark state, which we show to be less ordered than the photoproduct. NMR spectral analyses of the attached bilin chromophore are also consistent with this interpretation. NpF2164g3 is similar to the red/far-red phytochrome Cph1, which also has a more ordered chromophore-binding pocket in the photoproduct state;[37] however, NpF2164g3 is much less ordered than phytochromes in both photostates. NpF2164g3 also provides an interesting counterpoint to blue light sensors such as phototropins and photoactive yellow protein (PYP), in which light excitation leads to loss of ordered structure.[38, 39]

Results

NpF2164g3 is a monomer in solution. Compared to our previous characterization of the NpF2164g3 photoproduct state,[36] we found the signal-to-noise ratio was lower for the dark state and many peaks were broadened. One possible explanation would be a change from dimeric to monomeric NpF2164g3 upon photoproduct formation. The molar mass of NpF2164g3 in solution was therefore determined by measuring its molecular diffusion using NMR spectroscopy. A summary of ^{15}N NMR relaxation and heteronuclear NOE data for NpF2164g3 are presented in Fig. 3 (photoproduct, 3A-C; dark state, 3D and E). The average ^{15}N longitudinal relaxation rate constant (R_1) and ^{15}N transverse relaxation rate constant (R_2) from residues in structured regions were calculated as R_1 = 0.92 ±0.04 s^{-1} and R_2 = 23 ±1 s^{-1} for the light-activated state. For dark-state NpF2164g3, the average R_1 was 0.89 ±0.06 s^{-1} and average R_2 was 29 ±2 s^{-1}. Assuming isotropic tumbling of NpF2164g3, the overall rotational correlation time was obtained from R_1/R_2 ratios of all residues within 1 standard deviation of the average value.[40] Thus, the average rotational correlation time was calculated to be 16 ±1 ns (photoproduct) and 18 ±2 ns (dark state) at 300 K, consistent with NpF2164g3 as a protein monomer in solution. NMR pulsed-field gradient diffusion studies[41] estimated a translational diffusion coefficient D of 8.5 x 10^{-11} m^2/s for both dark and light-activated states. This D value is consistent with a molar mass of approximately 25 kDa, in good agreement with a calculated mass of 26 kDa for the NpF2164g3 monomer. The monomeric state of NpF2164g3 in solution differs from the oligomeric structures observed for phytochromes but is consistent with the monomeric behavior of the DXCF CBCR TePixJ in solution.[3-7, 35]

Secondary structure and conformational flexibility of the NpF2164g3 dark state. Figure S1 presents the HSQC spectrum of ^{15}N-labeled NpF2164g3 dark state to illustrate representative protein backbone resonance assignments. NMR assignments were based on 3D heteronuclear NMR experiments performed on ^{13}C/^{15}N-labeled NpF2164g3 (residues 463-664 of the full-length NpF2164 protein).[12] Approximately 75% of non-proline residues exhibited strong backbone amide resonances with uniform intensities, indicative of a stably folded protein structure for these residues. A total of 69% of backbone resonances (^{1}HN, ^{15}N, ^{13}Cα, ^{13}Cβ, and ^{13}CO) could be assigned (Figs. S1 and

4). The chemical shift assignments (^{1}H, ^{15}N, ^{13}C) of dark-state NpF2164g3 have been deposited in the BioMagResBank (http://www.bmrb.wisc.edu) under accession number 19629. Most of the unassigned resonances (residues 525-554, 589-599, and 654-660) exhibit weak NMR intensities with very broad linewidths, suggesting these residues are conformationally dynamic (see below).

We used chemical shift index[42] to assign protein secondary structure for dark-state NpF2164g3 (Figs. 1B and 4). The dark-state secondary structure is similar to that determined for the light-activated state.[36] However, there are three regions of the protein that exhibit light-dependent changes in secondary structure (Fig. 4): (1) the third helix in the light-activated state (residues 559-565) is a random coil in the dark state; (2) a large part of the 2nd Cys insert loop that resolved as random coil in the light-activated state is exchange broadened in the dark state (residues 530-554); (3) the C-terminal half of the fifth helix (residues 652-660) is stably helical in the light-activated state, but exchange broadened in the dark state. Using numbering based on the closest known CBCR structure, AnPixJ,[23] the secondary structure elements assigned for dark-state NpF2164g3 are α1: 470-476; α2: 481-495; β1: 499-505; β2: 513-519; β4: 575-582; β5: 603-609; β6: 618-624; α5A: 632-644; and α5B: 645-653. In all phytochrome and CBCR structures reported to date, the conserved CBCR Cys is located at the N-terminal end of a helix.[21, 23, 35] That helix is unstable or absent in NpF2164g3 (Fig. 1): in the photoproduct, the equivalent region adopts a random coil structure (residues 596-598), whereas these residues exhibited exchange broadened backbone resonances in the dark state and could not be assigned (residues 591-598; Fig. 4). The characteristic insertion loop of insert-Cys CBCRs (residues 523-559) exhibited a random coil chemical shift index for residues 528-529 and 555-559. Most of the insertion loop, *i.e.* residues 530-554, possessed exchange broadened backbone resonances, perhaps reflecting formation of metastable structure in this region. The remaining unassigned residues (490-492, 498-511, 525, and 577: Fig. 4) were not clearly resolved due to spectral overlap with other residues.

Surprisingly, the regions around both Cys546 and Cys591 are not associated with stable secondary structure in either photostate; however, important light-dependent structural differences in these regions can still be found. The behavior of these two regions is

correlated, as expected: the bilin atoms attached to Cys546 and Cys591 in the dark state ($C3^1$ and C10: Fig. 2) are only 7.5-8.3 Å apart in CBCR crystal structures.[21, 23] Fewer residues immediately adjacent to these two Cys residues remain unassigned for the light-activated state (residues 540-546 and 590-595) than for the dark state (530-554 and 590-598). Near the first Cys (Cys591), residues 596-598 are unassigned in the dark state yet exhibit well-defined random-coil peaks in the light-activated state. Similarly, residues in the insert-Cys insertion loop exhibited sharp, random-coil NMR peaks in the photoproduct state[36] but had very weak NMR intensities with ≥10-fold broader linewidths in the dark state. A chemical exchange process such as metastable secondary structure fluctuating on the millisecond timescale could cause this dark-state line broadening. The insert-Cys insertion loop therefore is not folded into a stable secondary structure in the dark state, despite the conformational constraint imposed upon this region by formation of the second linkage to the bilin. Elimination of the second linkage upon photoconversion removes this conformational constraint and allows large parts of the insertion loop to adopt the more flexible random coil observed in the light-activated state.[36] Thus, the characteristic insert-Cys insertion loop of NpF2164g3 is conformationally heterogeneous (millisecond dynamics) in the dark state while more flexible (nanosecond-picosecond dynamics) in the light-activated state.

Analysis of ^{15}N NMR relaxation parameters provides further support for light-dependent dynamics in the insert-Cys loop. The ^{15}N relaxation rate constants (R_1 and R_2) and heteronuclear NOE values for each assigned residue provide information about protein backbone dynamics in each photostate (Fig. 3). The NpF2164g3 residues in regions of regular secondary structure have relatively rigid backbone conformations, as indicated by large heteronuclear NOEs (>0.75) and R_2 values > 21 s^{-1} (Figs. 3 and 4). NpF2164g3 residues in random coil loop regions have considerable backbone flexibility, as indicated by relatively small heteronuclear NOEs (<0.65) and R_2 values < 20 s^{-1}. Most striking is the highly flexible backbone in the 2nd Cys insert loop region for light-activated NpF2164g3 (Fig. 3), as demonstrated by small heteronuclear NOEs (< 0.4), large R_1 values (>1 s^{-1}), and small R_2 values (<17 s^{-1}). By contrast, in dark-state NpF2164g3 (Fig. 3), most of the 2nd Cys insert loop (residues 530-544) was not assigned due to exchange broadening, indicating that this region is fluctuating on the millisecond timescale of

chemical shift values. The change in timescale of fluctuations likely reflects formation of the second linkage to the bilin, which would provide an additional constraint on the motions of this loop.

Our analysis of secondary structure in dark-state NpF2164g3 revealed an additional structural change occurring upon photoconversion: residues 559-565 adopt a random coil conformation in the dark state but fold into an α-helix (α3) in the light-activated state. This α-helix mirrors a short helical region (residues 92-98) in the crystal structure of the red-absorbing AnPixJ dark state (Figs. 1B and 4).[23] Indeed, residues 559-565 exhibit highly flexible backbone dynamics in the dark state (Fig. 3), as demonstrated by their small R_2 values (<15 s^{-1}) and large R_1 values (>1.2 s^{-1}). This is not observed for the same region in the NpF2164g3 photoproduct state, in which these residues instead form a stable α-helix.[36] This region includes Asp560 (Fig. 4, green), the conserved Asp-motif residue equivalent to those interacting with the bilin chromophore in several phytochrome and CBCR structures.[6, 21, 23] The corresponding residues in the dark-state AnPixJ crystal structure also form a stable α-helix,[23] with its Asp side-chain closest to the bilin A- and C-ring nitrogens and also contacting the B-ring nitrogen. The AnPixJ chromophore is sandwiched between this helix and the helix containing the conserved Cys residue attached to the A-ring (equivalent to Cys591 in NpF2164g3). Both of these helices are absent in the NpF2164g3 dark state.

Light-induced structural changes in the NpF2164g3 bilin chromophore. Our analysis of NpF2164g3 secondary structure implicated a less-ordered bilin in the dark state than in the photoproduct. To explore this hypothesis, we extended our solution NMR studies to NpF2164g3 samples containing isotopically labeled bilin chromophore. We first assessed protonation of the bilin chromophore by examining two samples: one containing ^{15}N protein and natural abundance bilin (>99% ^{14}N), and another containing both ^{15}N protein and ^{15}N bilin. Suppression of bilin signals with ^{14}N allowed unambiguous assignment of bilin NH moieties in two-dimensional ^{15}N-^{1}H HSQC NMR spectra by comparing the two samples (Fig. 5). In the dark state, nucleophilic addition of Cys546 to the bilin C10 atom produces a ring system that has four NH moieties but lacks a positive charge. Four NH crosspeaks would be present for such a neutral, fully protonated ring system. Elimination

of the second linkage would initially yield a protonated cationic ring system (Fig. 2) that could subsequently undergo deprotonation, as has been observed for some phytochromes and CBCRs.[43, 44] Thus, either three or four NH crosspeaks might be expected for the light-activated state.

The HSQC spectrum of light-activated NpF2164 exhibited four resonances that are suppressed by ^{14}N-labeled chromophore (Fig. 5B). Therefore, all four bilin nitrogen atoms are protonated in the orange-absorbing state, a result also consistent with the properties of denatured CBCRs at low pH.[43] The HSQC spectrum of dark-state NpF2164 exhibited only three resonances suppressed by ^{14}N-labeled chromophore (Fig. 5A, red). The integrated NMR intensity of the bilin resonance at 9.25 ppm (^{15}N: 145 ppm) is larger than that of the other two pyrrole resonances at 7.5 and 11.5 ppm (^{15}N: 143 and 134 ppm, respectively). Therefore, the peak at 9.25 ppm could represent two pyrrole resonances that are spectrally overlapped. However, it is also possible that the A-ring is sufficiently disordered such that its NH resonance is not detected due to proton exchange broadening. The latter interpretation is more consistent with changes in NpF2164g3 secondary structure upon photoconversion, as discussed above.

To gain more information about chromophore structure in NpF2164g3, we used 5-^{13}C aminolevulinic acid (5-^{13}C ALA) to label specific positions in the chromophore. ALA is the first committed precursor for synthesis of heme, which is converted to the NpF2164g3 chromophore PCB for these studies using an engineered *E. coli* strain.[45] With incorporation of 5-^{13}C ALA, a subset of carbon atoms in PCB are labeled: C4, C5, C9, C10, C11, C15, and C19 (Fig. 2). This labeling approach requires growth of *E. coli* in minimal media to ensure efficient incorporation of 5-^{13}C ALA, which has proven successful for the DXCF CBCR TePixJ.[46] We found that chromophore incorporation in this system was poor for NpF2164g3. Poor chromophore incorporation led to low signal-to-noise ratio (S/N) for the chromophore due to low concentrations of holoprotein and large amounts of apoprotein, precluding acquisition of two-dimensional ^{13}C-^{1}H spectra. Proton-decoupled one-dimensional ^{13}C spectra (Fig. 6) and ^{13}C-^{1}H INEPT spectra (Fig. S2) were successfully obtained for both photostates. ^{13}C-^{1}H INEPT spectra only detect resonances for ^{13}C atoms attached to hydrogen, identifying the bridge atoms C5, C10, and

C15. Combining the INEPT spectra with the one-dimensional ^{13}C chemical shifts and C–C splitting patterns allowed assignment of all labeled carbons with the exception of C9 and C11, which could not be reliably distinguished from each other because of their very similar chemical environments and because both are adjacent to the C10 atom. The resulting assignments are reported in Table 1.

The largest light-induced spectral change was observed for the ^{13}C resonance assigned to the C10 position. In the dark-state, the C10 resonance exhibited a ^{13}C chemical shift of 34.5 ppm (Fig. 6B), consistent with a methylene carbon. In the light-activated state, the C10 resonance exhibited a ^{13}C chemical shift of 116 ppm (Fig. 6A), indicative of a methine carbon. The change in C10 chemical shift is much larger than any other such change in the labeled carbons (Table 1), providing direct spectroscopic support for elimination of the second linkage in the *15E* light-activated state. This result corroborates previous site-directed mutagenesis and biochemical studies.[12]

Photoconversion of NpF2164g3 resulted in changes for ^{13}C resonances assigned to other carbons as well (Fig. 6 and Table 1). C15 and C19 were both shifted upfield in the light-activated state relative to the dark state, as has been reported for red/far-red phytochromes.[16] C9 and C11 were not resolved from each other. Two resonances were assigned to these atoms in the light-activated state, but only one was resolved above natural abundance signals in the dark state (Fig. 6 and Table 1). Similarly, C4 was clearly resolved in the light-activated state but was not resolved in the dark state. These results are consistent with conformationally flexible bilin A- and B-rings in the dark state. Further support for this hypothesis comes from the C5 resonance. C5 exhibited a well-resolved doublet in the photoproduct state but a broader, weak peak in the dark state (Fig. 6). Taken together, our ^{13}C and ^{15}N chromophore studies resolve resonances from all four rings in the light-activated state but fail to resolve the A-ring unambiguously in the dark state. These results are consistent with the protein NMR spectra implicating the dark state structure to be poorly ordered in the vicinity of the A- and B-rings.

Discussion

In this study, we present NMR chemical shift assignments of the NpF2164g3 dark state and detailed spectral analysis of the bilin chromophore. On the basis of our NMR assignments, the overall secondary structure of the dark state is similar to that of the photoproduct, except that helices (α3 and α5b) in the photoproduct becomes random coil in the dark state and residues in the 2nd Cys insert loop region are exchange broadened in the dark state (Fig. 4). We interpret the NMR results to indicate that the NpF2164g3 dark state may exhibit multiple partially folded configurations fluctuating on the chemical shift timescale (milliseconds), with a stably folded central β sheet. Neither Cys residue attached to the NpF2164g3 chromophore in the dark state is in a stably folded structural element, so we propose that the bilin A- and B-rings exhibit conformational flexibility in the dark state. This is also consistent with the exchange broadened dark-state resonance for the C4 atom and with the poorly resolved dark-state resonance for the C5 atom (Fig. 6 and Table 1). Elimination of the second Cys–bilin linkage upon photoconversion leads to faster dynamics about the two Cys residues in the photoproduct. The Asp-motif also folds into a stable helix in the photoproduct, implicating a more ordered Asp560 sidechain and hence a more ordered bilin B-ring. Thus, we propose that the dark state provides a 'half pocket' for the bilin chromophore, with only the C- and D-rings surrounded by stable protein structure. Photoconversion would then provide a more ordered protein structure that also envelops the B-ring. This interpretation of NpF2164g3 structure contrasts with structural changes observed upon photoconversion in other sensors for violet and blue light. In phototropin, photoconversion leads to helix unfolding in the light-activated state, whereas in the CBCR TePixJ the helical structure of the Asp-motif is present in the dark state but lost in the photoproduct.[21, 23, 35, 39]

Light-dependent protein conformational changes in NpF2164g3. NMR chemical shift assignments of protein resonances for dark-state (Fig. S1) and photoproduct[36] NpF2164g3 were used to calculate the light-induced chemical shift difference (CSD) for each residue. CSD was calculated as $[(H_N^D - H_N^L)^2 + (^{15}N^D - ^{15}N^L)^2]^{1/2}$ where H_N^D and $^{15}N^D$ are amide ^1H and ^{15}N chemical shifts in the dark state, and H_N^L and $^{15}N^L$ are amide ^1H and ^{15}N chemical shifts in the photoproduct state.[36] The CSD for each residue is

plotted in Fig. 7. The largest CSD values are observed for residues 555-575, comprising the end of the 2nd Cys insert loop and the adjacent region forming α3 in the photoproduct. As discussed above, the light-dependent folding of α3 explains why these residues have such large CSD values. Four residues immediately upstream from α3 (residues 555-559) also exhibit large light-dependent spectral changes. Residues 555-575 therefore undergo light-dependent structural changes.

We speculate that the remaining 2nd Cys insert loop residues (529-555) also undergo light-dependent structural changes, because many of these residues show striking light-dependent linewidths. Unfortunately, broad NMR resonances for residues 530-554 prevent definitive NMR assignments of this region in the dark state. Broad NMR resonances were also observed in the dark state for residues 590-598, flanking the 1st Cys attachment site, and for residues 652-660 near the C-terminus. Covalent attachment of the bilin to both Cys546 and Cys591 thus appears to trigger structural heterogeneity and/or conformational dynamics of the dark-state at these sites. Moderate CSD values were also seen for residues 515-520 in β2, suggesting that β2 is structurally coupled to the light-dependent structural changes in the adjacent 2nd Cys insert loop (Fig. 1B). The remaining assigned NMR resonances are found mainly in regions of stable secondary structure throughout the protein (Fig. 4). These residues exhibit relatively small CSD values, suggesting that these residues do not undergo major changes upon light activation. Therefore, the largest CSD values are attributable to residues in the vicinity of the two Cys residues and to those in the C-terminal half of α5B in the photoproduct state.

Like helix α3, helix α5B is only stable in the light-activated state. Based on the AnPixJ crystal structure,[23] the residues comprising α5B are expected to be > 20Å distant from the three other regions exhibiting substantial structural changes upon photoconversion (α3 and the loops surrounding Cys546 and Cys591). Like α1 and α2, α5 is one of three 'back-side helices' on the opposite side of the central GAF β sheet from the chromophore. Such a change in distant secondary structure is well-established in flavin-based blue light sensors such as phototropin.[39] Indeed, light-induced unfolding of the Jα helix is implicated in phototropin signaling to downstream effectors C-terminal to the

photosensor.[47] Phototropin is thus reversed relative to NpF2164g3, in which α5B is distant from the chromophore, but undergoes light-induced folding rather than unfolding. A similar extension of the α5 helix upon photoconversion is observed in TePixJ, even though light-dependent structural changes at α3 are reversed in this protein relative to NpF2164g3.[35]

Possible implications for conserved CBCR signaling mechanisms. An unanswered question in phytochrome research is how structural changes in the vicinity of the chromophore are transmitted to the biologically active signaling 'output' domains.[2, 5, 6, 8, 37] Recent studies have centered on models involving transmission of signal via a conserved 'tongue' in the phytochrome PHY domain immediately C-terminal to the chromophore binding GAF domain or models involving changes in the interface between the two molecules of a dimeric phytochrome photosensor., in turn changing the properties of a dimeric output domain.[5, 6, 8, 48] CBCRs do not possess PHY domains, so signal propagation via a tongue cannot take place. The CBCR TePixJ is monomeric in solution even at high concentrations, so its dimerization affinity must be low.[35] In this work, we find that NpF2164g3 is also monomeric. It thus seems that at least a subset of CBCRs are not dimeric, implying that signal propagation in such CBCRs must differ from that in phytochromes. However, CBCR output domains usually belong to protein families such as histidine kinases or GGDEF domains,[49] which must dimerize to function. We therefore sought to develop a hypothetical yet testable model that might explain how a monomeric CBCR domain could influence the properties of a potentially dimeric output domain. As a first step, we compared changes in secondary structure upon photoconversion in the two CBCRs for which solution structures are available, [35] TePixJ and NpF2164g3 (Fig. 1). At this level of resolution, the change upon photoconversion that is conserved in these two proteins is an extension of the C-terminal α5 helix in the photoproduct state.

We therefore speculate that the light-dependent folding and unfolding of the α5B helix could be a signaling mechanism shared by NpF2164g3 and TePixJ. It is known that the back-side helices provide a dimerization interface for phytochrome photosensors.[3-6] Even though NpF2164g3 is monomeric as an isolated CBCR domain, it is one of several CBCR domains in tandem within the full-length NpF2164 protein.[12, 20] Folding and

unfolding of α5B could influence the dimerization affinity of adjacent domains, for example by producing a continuous helix with α1 in NpF2164g4. In the general case, subtle structural changes could be passed to a C-terminal signaling 'output' domain down a chain of tandem CBCR domains, an arrangement commonly found in cyanobacteria.[49] In this model, shown conceptually for a two-domain tandem sensor in Fig. 8, changes in activity of the output domain would be modulated by photoconversion of intrinsically monomeric CBCRs because the folding and unfolding of α5 would potentiate formation or disruption of output-domain dimers. This model provides a possible explanation for the function of tandem CBCR sensors and may also explain why the output domains for such proteins are typically located at the C-terminus.[49] It also is consistent with modulation of signaling activity by tandem CBCR sensors in the few cases reported to date.[50, 51]

Conclusions. These NMR studies on the insert-Cys CBCR NpF2164g3 elucidate light-dependent structural changes in both the protein and bilin. NMR relaxation analysis demonstrates that NpF2164g3 is a protein monomer in solution, in contrast to the dimeric crystal structures observed for bacterial phytochromes.[2-7] NMR spectra of NpF2164g3 containing a ^{15}N-labeled bilin indicate that all four pyrrole nitrogen atoms are protonated in both the dark-adapted and light-activated photostates. Light-dependent NMR spectral changes assigned to the bilin C10 atom fully corroborate the predicted covalent attachment of Cys546 to the bilin.[12] NMR assignments of protein backbone resonances indicate an overall similar protein secondary structure for the dark state and light-activated state. However, an additional α-helix (residues 559-565) is only formed after photoconversion to the light-activated state. While exchange broadened in the dark state, the characteristic insertion loop region of the insert-Cys CBCRs (residues 528-558) forms a highly flexible random coil in the light-activated state. The C-terminal half of α5b (residues 652-660) adopts a stable helical conformation in the NpF2164g3 photoproduct state, which becomes exchange broadened in the dark-state. Overall, the dark state is less folded than the photoproduct state, with no evidence for a well-ordered pocket binding the chromophore A-ring in the dark state. One helix found in all other CBCR and

phytochrome structures to date is absent in NpF2164g3 in both photostates. These studies thus implicate unanticipated structural diversity in the phytochrome superfamily.

Experimental

Expression and Purification of NpF2164g3. The protein sample in this study consists of 201 native residues with an N-terminal His-tag (MGSSHHHHHHSSGLVPRGSHM). Expression and purification of NpF2164g3 used co-production of PCB in *E. coli* grown in commercial ^{15}N- or ^{15}N/^{13}C-labeled rich media (BioExpress, Cambridge Isotopes), followed by purification on Ni-NTA resin with elution using an imidazole gradient.[36] Peak fractions were pooled for overnight dialysis into 10 mM sodium phosphate (pH 7.4) supplemented with 1 mM EDTA to remove residual metal ions followed by final overnight dialysis into 10 mM sodium phosphate (pH 7.4). NMR samples of dark-state NpF2164g3 were prepared by concentrating the peak fractions to a final protein concentration of 0.7 mM; D_2O was then added to 7% (v/v). NMR samples of the light-activated state were generated by illuminating the sample with a 405 nm class IIIa laser pointer (LightVision Technologies) to photoequilibrium, with the orange-absorbing state present at 85%.[36] The reverse reaction was triggered using a 75W xenon source passed through a water filter and a 600±20 nm bandpass intereference filter as described.[12] Subsequent manipulations were performed in darkness. For NMR characterization of the orange state, 1.2 mM deuterated *tris*-carboxyethyl phosphine (Cambridge Isotopes) was added to suppress oxidation of the insert-Cys cysteine.

Preparation of NpF2164g3 with differentially labeled bilin. For specific labeling of bilin, expression was performed in M9 minimal media containing ^{15}N ammonium chloride and supplemented with ALA, followed by purification as described above. For partial ^{13}C labeling of the bilin chromophore, 5-^{13}C ALA (Sigma) was added to a final concentration of approximately 100 μM.[46] For suppression of ^{15}N incorporation, natural abundance ALA (Sigma) was added to a final concentration of approximately 1 mM, which was empirically determined to suppress the four bilin NH crosspeaks in the HSQC spectrum of the photoproduct state.

NMR spectroscopy. NMR experiments were conducted using a Bruker Advance 600 MHz spectrometer equipped with a triple resonance cryogenic probe. All experiments were performed in darkness, with spectral acquisition at 303 K. Backbone chemical shift assignments were obtained using ^{1}H,^{15}N-HSQC, HNCA, HNCO, HNCACB, HNCACO, CBCACONH, HBHACONH, ^{1}H,^{15}N-HSQC-TOCSY (mixing time of 60 ms), and ^{1}H,^{15}N-NOESY-HSQC (mixing time of 120 ms) spectra.[52] NMR data were processed using the NMRPipe software package[53] and analyzed using SPARKY (www.cgl.ucsf.edu/home/sparky).

^{15}N NMR Relaxation Measurements. ^{15}N R_1, R_2, and [^{1}H]-^{15}N NOE experiments were performed on NpF2164g3 at 30°C using standard pulse sequences described previously.[54] Longitudinal magnetization decay was recorded using seven different delay times: 0.01, 0.05, 0.15, 0.2, 0.3, 0.4, and 0.8 s. Transverse magnetization decay was recorded with eight different delays: 0.0, 0.016, 0.032, 0.048, 0.064, 0.08, 0.096, and 0.112 s. To check sample stability, transverse magnetization decay at 0.032 s was verified to be unchanged before and after each set of measurements. A recycle delay of 1.5 s was employed in measurements of both ^{15}N R_1 and R_2 experiments. Steady-state [^{1}H]-^{15}N NOE values were obtained by recording two sets of spectra in the presence and absence of a 3 s proton saturation period. The NOE experiments were repeated three times to calculate average and standard deviation of the NOE values. The overall rotational correlation time for backbone amide motion was determined using the protocol described previously.[55]

Acknowledgements

This work was supported by a grant from the Chemical Sciences, Geosciences, and Biosciences Division, Office of Basic Energy Sciences, Office of Science, United States Department of Energy (DOE DE-FG02-09ER16117 to J.C.L. and J.B.A.), with partial support for NMR time from NIH grant RR11973 to the UC Davis NMR facility. NMR time for pilot experiments was supported by NIH grant EY012347 to J.B.A.

References

1. K.-C. Yeh, S.-H. Wu, J. T. Murphy and J. C. Lagarias, A cyanobacterial phytochrome two-component light sensory system. *Science*, 1997, **277**, 1505-1508.
2. J. R. Wagner, J. S. Brunzelle, K. T. Forest and R. D. Vierstra, A light-sensing knot revealed by the structure of the chromophore binding domain of phytochrome. *Nature*, 2005, **438**, 325-331.
3. J. R. Wagner, J. Zhang, J. S. Brunzelle, R. D. Vierstra and K. T. Forest, High resolution structure of *Deinococcus* bacteriophytochrome yields new insights into phytochrome architecture and evolution. *J. Biol. Chem.*, 2007, **282**, 12298-12309.
4. X. Yang, E. A. Stojkovic, J. Kuk and K. Moffat, Crystal structure of the chromophore binding domain of an unusual bacteriophytochrome, RpBphP3, reveals residues that modulate photoconversion. *Proc. Natl. Acad. Sci. USA*, 2007, **104**, 12571-12576.
5. L. O. Essen, J. Mailliet and J. Hughes, The structure of a complete phytochrome sensory module in the Pr ground state. *Proc. Natl. Acad. Sci. USA*, 2008, **105**, 14709-14714.
6. X. Yang, J. Kuk and K. Moffat, Crystal structure of *Pseudomonas aeruginosa* bacteriophytochrome: photoconversion and signal transduction. *Proc. Natl. Acad. Sci. USA*, 2008, **105**, 14715-14720.
7. D. Bellini and M. Z. Papiz, Structure of a bacteriophytochrome and light-stimulated protomer swapping with a gene repressor. *Structure*, 2012, **20**, 1436-1446.
8. K. Anders, G. Daminelli-Widany, M. A. Mroginski, D. von Stetten and L. O. Essen, Structure of the cyanobacterial phytochrome 2 photosensor implies a tryptophan switch for phytochrome signaling. *J. Biol. Chem.*, 2013, **288**, 35714-35725.
9. M. Ikeuchi and T. Ishizuka, Cyanobacteriochromes: a new superfamily of tetrapyrrole-binding photoreceptors in cyanobacteria. *Photochem. Photobiol. Sci.*, 2008, **7**, 1159-1167.
10. N. C. Rockwell and J. C. Lagarias, A brief history of phytochromes. *ChemPhysChem*, 2010, **11**, 1172-1180.
11. M. E. Auldridge and K. T. Forest, Bacterial phytochromes: More than meets the light. *Crit. Rev. Biochem. Mol. Biol.*, 2011, **46**, 67-88.
12. N. C. Rockwell, S. S. Martin, K. Feoktistova and J. C. Lagarias, Diverse two-cysteine photocycles in phytochromes and cyanobacteriochromes. *Proc. Natl. Acad. Sci. USA*, 2011, **108**, 11854-11859.
13. V. Sineshchekov, L. Koppel, B. Esteban, J. Hughes and T. Lamparter, Fluorescence investigation of the recombinant cyanobacterial phytochrome (Cph1) and its C-terminally truncated monomeric species (Cph1Delta2): implication for holoprotein assembly, chromophore-apoprotein interaction and photochemistry. *J. Photochem. Photobiol. B.*, 2002, **67**, 39-50.
14. J. Hughes, Phytochrome three-dimensional structures and functions. *Biochem. Soc. Trans.*, 2010, **38**, 710-716.

15. T. Ishizuka, A. Kamiya, H. Suzuki, R. Narikawa, T. Noguchi, T. Kohchi, K. Inomata and M. Ikeuchi, The cyanobacteriochrome, TePixJ, isomerizes its own chromophore by converting phycocyanobilin to phycoviolobilin. *Biochemistry*, 2011, **50**, 953-961.
16. C. Song, G. Psakis, C. Lang, J. Mailliet, W. Gartner, J. Hughes and J. Matysik, Two ground state isoforms and a chromophore D-ring photoflip triggering extensive intramolecular changes in a canonical phytochrome. *Proc. Natl. Acad. Sci. USA*, 2011, **108**, 3842-3847.
17. X. Yang, Z. Ren, J. Kuk and K. Moffat, Temperature-scan cryocrystallography reveals reaction intermediates in bacteriophytochrome. *Nature*, 2011, **479**, 428-432.
18. P. W. Kim, L. H. Freer, N. C. Rockwell, S. S. Martin, J. C. Lagarias and D. S. Larsen, Second-Chance Initiation Dynamics of the Cyanobacterial Photocycle in the NpR6012 GAF4 Domain of *Nostoc Punctiforme*. *J. Am. Chem. Soc.*, 2012, **134**, 130-133.
19. N. C. Rockwell, S. S. Martin, A. G. Gulevich and J. C. Lagarias, Phycoviolobilin formation and spectral tuning in the DXCF cyanobacteriochrome subfamily. *Biochemistry*, 2012, **51**, 1449-1463.
20. N. C. Rockwell, S. S. Martin and J. C. Lagarias, Red/Green Cyanobacteriochromes: Sensors of Color and Power. *Biochemistry*, 2012, **51**, 9667-9677.
21. E. S. Burgie, J. M. Walker, G. N. Phillips, Jr. and R. D. Vierstra, A photo-labile thioether linkage to phycoviolobilin provides the foundation for the blue/green photocycles in DXCF-cyanobacteriochromes. *Structure*, 2013, **21**, 88-97.
22. P. W. Kim, N. C. Rockwell, L. H. Freer, C. W. Chang, S. S. Martin, J. C. Lagarias and D. S. Larsen, Unraveling the Primary Isomerization Dynamics in Cyanobacterial Phytochrome Cph1 with Multi-pulse Manipulations. *J. Phys. Chem. Lett.*, 2013, **4**, 2605-2609.
23. R. Narikawa, T. Ishizuka, N. Muraki, T. Shiba, G. Kurisu and M. Ikeuchi, Structures of cyanobacteriochromes from phototaxis regulators AnPixJ and TePixJ reveal general and specific photoconversion mechanism. *Proc. Natl. Acad. Sci. USA*, 2013, **110**, 918-923.
24. C. Song, G. Psakis, J. Kopycki, C. Lang, J. Matysik and J. Hughes, The D-ring, not the A-ring, Rotates in Synechococcus OS-B' Phytochrome. *J. Biol. Chem.*, 2013, **289**, 2552-2562.
25. F. Velazquez Escobar, T. Utesch, R. Narikawa, M. Ikeuchi, M. A. Mroginski, W. Gartner and P. Hildebrandt, Photoconversion Mechanism of the Second GAF Domain of Cyanobacteriochrome AnPixJ and the Cofactor Structure of Its Green-Absorbing State. *Biochemistry*, 2013, **52**, 4871-4880.
26. N. C. Rockwell, Y. S. Su and J. C. Lagarias, Phytochrome structure and signaling mechanisms. *Ann. Rev. Plant Biol.*, 2006, **57**, 837-858.
27. L. H. Freer, P. W. Kim, S. C. Corley, N. C. Rockwell, L. Zhao, A. J. Thibert, J. C. Lagarias and D. S. Larsen, Chemical inhomogeneity in the ultrafast dynamics of the DXCF cyanobacteriochrome Tlr0924. *J Phys Chem B*, 2012, **116**, 10571-10581.

28. S. M. Gottlieb, P. W. Kim, N. C. Rockwell, Y. Hirose, M. Ikeuchi, J. C. Lagarias and D. S. Larsen, Primary photodynamics of the green/red-absorbing photoswitching regulator of the chromatic adaptation E domain from Fremyella diplosiphon. *Biochemistry*, 2013, **52**, 8198-8208.
29. S. M. Gottlieb, P. W. Kim, S. C. Corley, D. Madsen, S. J. Hanke, C. W. Chang, N. C. Rockwell, S. S. Martin, J. C. Lagarias and D. S. Larsen, Primary and Secondary Photodynamics of the Violet/Orange Dual-Cysteine NpF2164g3 Cyanobacteriochrome Domain from Nostoc punctiforme. *Biochemistry*, 2014, **53**, 1029-1040.
30. T. Dammeyer and N. Frankenberg-Dinkel, Function and distribution of bilin biosynthesis enzymes in photosynthetic organisms. *Photochemical and Photobiological Sciences*, 2008, **7**, 1121-1130.
31. G. Enomoto, Y. Hirose, R. Narikawa and M. Ikeuchi, Thiol-based photocycle of the blue and teal light-sensing cyanobacteriochrome Tlr1999. *Biochemistry*, 2012, **51**, 3050-3058.
32. Q. Ma, H. H. Hua, Y. Chen, B. B. Liu, A. L. Kramer, H. Scheer, K. H. Zhao and M. Zhou, A rising tide of blue-absorbing biliprotein photoreceptors: characterization of seven such bilin-binding GAF domains in *Nostoc* sp. PCC7120. *FEBS J.*, 2012, **279**, 4095-4108.
33. N. C. Rockwell, S. L. Njuguna, L. Roberts, E. Castillo, V. L. Parson, S. Dwojak, J. C. Lagarias and S. C. Spiller, A second conserved GAF domain cysteine is required for the blue/green photoreversibility of cyanobacteriochrome Tlr0924 from *Thermosynechococcus elongatus*. *Biochemistry*, 2008, **47**, 7304-7316.
34. N. C. Rockwell, S. S. Martin and J. C. Lagarias, Mechanistic Insight into the Photosensory Versatility of DXCF Cyanobacteriochromes. *Biochemistry*, 2012, **51**, 3576-3585.
35. C. C. Cornilescu, G. Cornilescu, E. S. Burgie, J. L. Markley, A. T. Ulijasz and R. D. Vierstra, Dynamic Structural Changes Underpin Photoconversion of a Blue/Green Cyanobacteriochrome Between its Dark and Photoactivated States. *J. Biol. Chem.*, 2013.
36. S. Lim, N. C. Rockwell, S. S. Martin, J. C. Lagarias and J. B. Ames, ^{1}H, ^{15}N, and ^{13}C chemical shift assignments of cyanobacteriochrome NpF2164g3 in the photoproduct state. *Biomolecular NMR Assignments*, 2013.
37. C. Song, G. Psakis, C. Lang, J. Mailliet, J. Zaanen, W. Gartner, J. Hughes and J. Matysik, On the collective nature of phytochrome photoactivation. *Biochemistry*, 2011, **50**, 10987-10989.
38. M. E. van Brederode, W. D. Hoff, I. H. van Stokkum, M. L. Groot and K. J. Hellingwerf, Protein folding thermodynamics applied to the photocycle of the photoactive yellow protein. *Biophys. J.*, 1996, **71**, 365-380.
39. S. M. Harper, L. C. Neil and K. H. Gardner, Structural basis of a phototropin light switch. *Science*, 2003, **301**, 1541-1544.
40. D. Marion, P. C. Driscoll, L. E. Kay, P. T. Wingfield, A. Bax, A. M. Gronenborn and G. M. Clore, Overcoming the overlap problem in the assignment of 1H NMR spectra of larger proteins by use of three-dimensional heteronuclear 1H-15N Hartmann-Hahn-multiple quantum coherence and nuclear Overhauser-multiple

quantum coherence spectroscopy: application to interleukin 1 beta. *Biochemistry*, 1989, **28**, 6150-6156.

41. A. S. Altieri, D. P. Hinton and R. A. Byrd, Association of Biomolecular Systems Via Pulsed-Field Gradient Nmr Self-Diffusion Measurements. *J. Am. Chem. Soc.*, 1995, **117**, 7566-7567.
42. D. S. Wishart, B. D. Sykes and F. M. Richards, The chemical shift index: a fast and simple method for the assignment of protein secondary structure through NMR spectroscopy. *Biochemistry*, 1992, **31**, 1647-1651.
43. Y. Hirose, N. C. Rockwell, K. Nishiyama, R. Narikawa, Y. Ukaji, K. Inomata, J. C. Lagarias and M. Ikeuchi, Green/red cyanobacteriochromes regulate complementary chromatic acclimation via a protochromic photocycle. *Proc. Natl. Acad. Sci. USA*, 2013, **110**, 4974-4979.
44. B. Zienicke, I. Molina, R. Glenz, P. Singer, D. Ehmer, F. Velazquez Escobar, P. Hildebrandt, R. Diller and T. Lamparter, Unusual spectral properties of bacteriophytochrome Agp2 result from a deprotonation of the chromophore in the red-absorbing form Pr. *J. Biol. Chem.*, 2013, **288**, 31738-31751.
45. K. Mukougawa, H. Kanamoto, T. Kobayashi, A. Yokota and T. Kohchi, Metabolic engineering to produce phytochromes with phytochromobilin, phycocyanobilin, or phycoerythrobilin chromophore in *Escherichia coli*. *FEBS Lett.*, 2006, **580**, 1333-1338.
46. A. T. Ulijasz, G. Cornilescu, D. von Stetten, C. Cornilescu, F. Velazquez Escobar, J. Zhang, R. J. Stankey, M. Rivera, P. Hildebrandt and R. D. Vierstra, Cyanochromes are blue/green light photoreversible photoreceptors defined by a stable double cysteine linkage to a phycoviolobilin-type chromophore. *J. Biol. Chem.*, 2009, **284**, 29757-29772.
47. S. M. Harper, J. M. Christie and K. H. Gardner, Disruption of the LOV-Jalpha helix interaction activates phototropin kinase activity. *Biochemistry*, 2004, **43**, 16184-16192.
48. A. Möglich, X. Yang, R. A. Ayers and K. Moffat, Structure and function of plant photoreceptors. *Ann. Rev. Plant Biol.*, 2010, **61**, 21-47.
49. C. Mandalari, A. Losi and W. Gärtner, Distance-tree analysis, distribution and co-presence of bilin- and flavin-binding prokaryotic photoreceptors for visible light. *Photochem. Photobiol. Sci.*, 2013, **12**, 1144-1157.
50. Y. Chen, J. Zhang, J. Luo, J. M. Tu, X. L. Zeng, J. Xie, M. Zhou, J. Q. Zhao, H. Scheer and K. H. Zhao, Photophysical diversity of two novel cyanobacteriochromes with phycocyanobilin chromophores: photochemistry and dark reversion kinetics. *FEBS J.*, 2012, **279**, 40-54.
51. A. N. Bussell and D. M. Kehoe, Control of a four-color sensing photoreceptor by a two-color sensing photoreceptor reveals complex light regulation in cyanobacteria. *Proc. Natl. Acad. Sci. USA*, 2013, **110**, 12834-12839.
52. M. Ikura, L. E. Kay and A. Bax, A novel approach for sequential assignment of ^{1}H, ^{13}C, and ^{15}N spectra of proteins: heteronuclear triple-resonance three-dimensional NMR spectroscopy. Application to calmodulin. *Biochemistry*, 1990, **29**, 4659-4667.

53. F. Delaglio, S. Grzesiek, G. W. Vuister, G. Zhu, J. Pfeifer and A. Bax, NMRPipe: a multidimensional spectral processing system based on UNIX pipes. *J. Biomol. NMR*, 1995, **6**, 277-293.
54. N. A. Farrow, R. Muhandiram, A. U. Singer, S. M. Pascal, C. M. Kay, G. Gish, S. E. Shoelson, T. Pawson, J. D. Forman-Kay and L. E. Kay, Backbone dynamics of a free and phosphopeptide-complexed Src homology 2 domain studied by 15N NMR relaxation. *Biochemistry*, 1994, **33**, 5984-6003.
55. D. I. Freedberg, R. Ishima, J. Jacob, Y. X. Wang, I. Kustanovich, J. M. Louis and D. A. Torchia, Rapid structural fluctuations of the free HIV protease flaps in solution: relationship to crystal structures and comparison with predictions of dynamics calculations. *Protein Science*, 2002, **11**, 221-232.

Table 1: ^{13}C Resonances in NpF2164g3[a]

Atom	δ_C (*15Z* dark state, ppm)	δ_C (*15E* photoproduct, ppm)
C4	N/R	150 (d)
C5	95.5 (m)	92 (d)
C9[2]	125.5? (d)	127 (d) or 128 (d)
C10	34.5 (m)	116 (m)
C11[b]	125.5? (d)	127 (d) or 128 (d)
C15	100.5 (s)	98 (s)
C19	172 (s)	171 (s)

a. Assignments made based on chemical shift value, C–C splitting pattern, and ^{13}C-^{1}H INEPT spectra as discussed in the text. N/R, not resolved. All chemical shift values are reported relative to TMS standard. Splitting patterns are reported as s, singlet; d, doublet; m, broad multiplet.

b. In the *15Z* state, only one resonance was clearly resolved in the C9/C11 region, designated with a '?' character. In the *15E* state, two resonances were observed. It was not possible to assign these peaks to C9 or C11 unambiguously for either photostate.

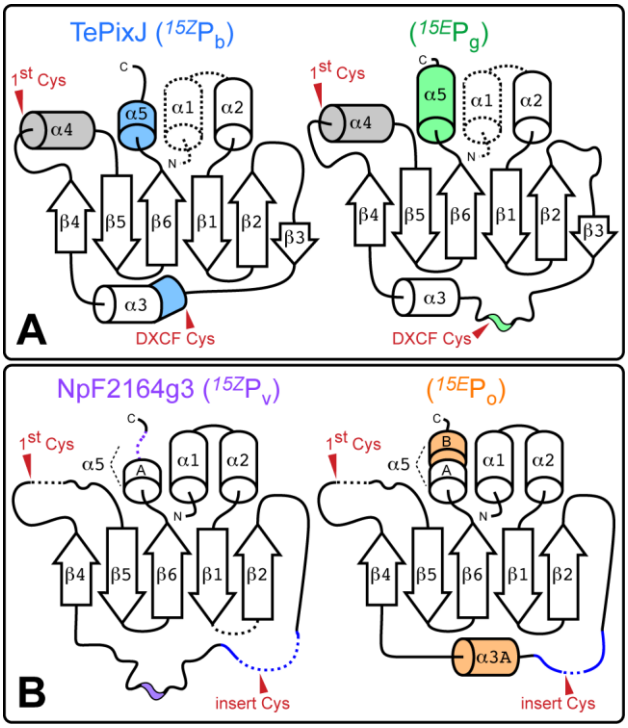

Fig. 1 Changes in CBCR secondary structure upon photoconversion. (A) Topology diagrams for the DXCF CBCR TePixJ[21, 23, 35] based on solution structures of the blue-absorbing dark state (*left)* and green-absorbing photoproduct (*right)*.[35] (B) Topology diagrams for the insert-Cys CBCR NpF2164g3 as violet-absorbing dark state (*left*, this work) and orange-absorbing photoproduct[36] (*right*). For NpF2164g3, the insert-Cys CBCR insertion loop (blue) is highlighted. For both proteins, critical Cys residues (red) are highlighted, regions not resolved in NMR secondary structure determination are dashed, and the α4 helix containing the Cys covalently linked to the bilin A-ring (Cys591 in NpF2164g3) is shaded grey where present.

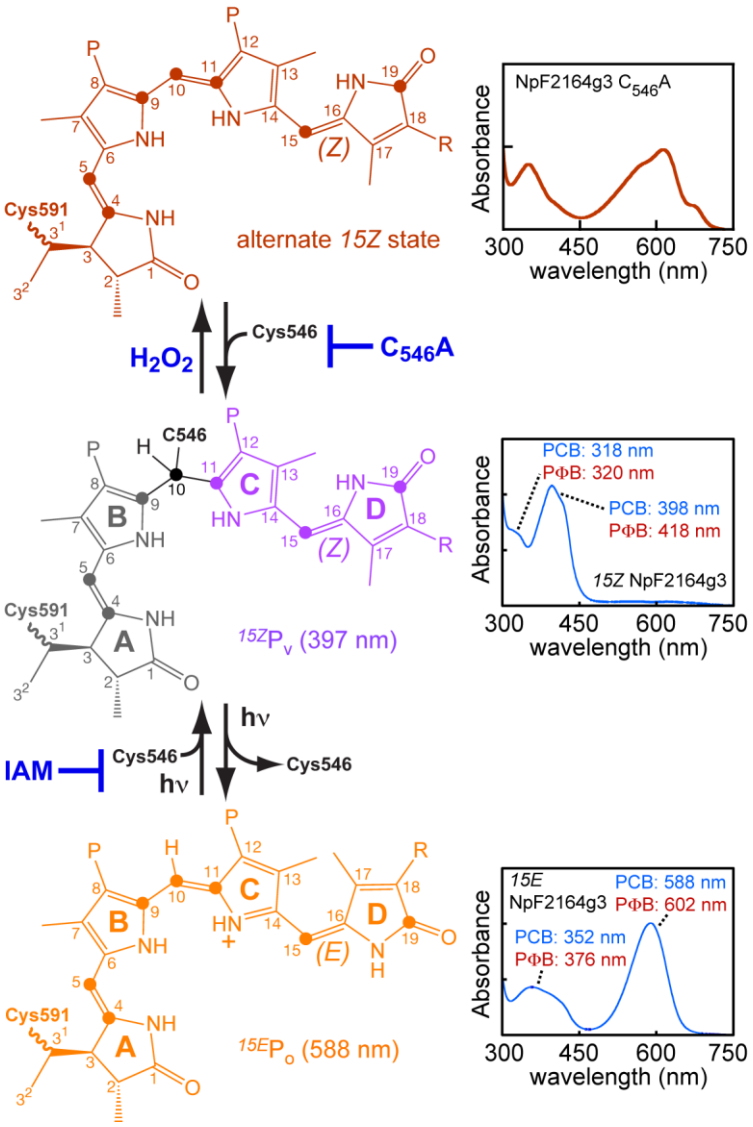

Fig. 2 The violet/orange photocycle of NpF2164g3. Bilin chromophore structures are shown on the left, absorption spectra are shown on the right, and experimental perturbations of the photocycle are highlighted in blue. IAM, iodoacetamide. The C18 sidechain varies with bilin (phycocyanobilin or PCB, R=Et; phytochromobilin or PΦB, R=Vn). A *15Z* red-absorbing state *(top)* is observed experimentally upon mutation of Cys546 or upon treatment of the $^{15Z}P_V$ dark state with hydrogen peroxide. In wild-type NpF2164g3, the $^{15Z}P_V$ dark state is formed *(middle)*. In the $^{15Z}P_V$ state, Cys546 is covalently attached to the bilin C10 atom. This splits the conjugated system of the bilin chromophore in two. The system formed by the C- and D-rings exhibits a red-shift with PΦB, while that formed by the A- and B-rings does not.[12] Photoisomerization of the

15,16-double bond leads to elimination of the second linkage, restoring conjugation across the C10 methine bridge in the $^{15E}P_o$ state (*bottom)*. Carbons, rings, and the configuration of the 15,16-double bond are indicated. Filled circles indicate carbon atoms labeled by bilin biosynthesis using 5-^{13}C ALA. Grey, purple, and orange indicate conjugated systems absorbing at 322, 397, and 588 nm, respectively.[12]

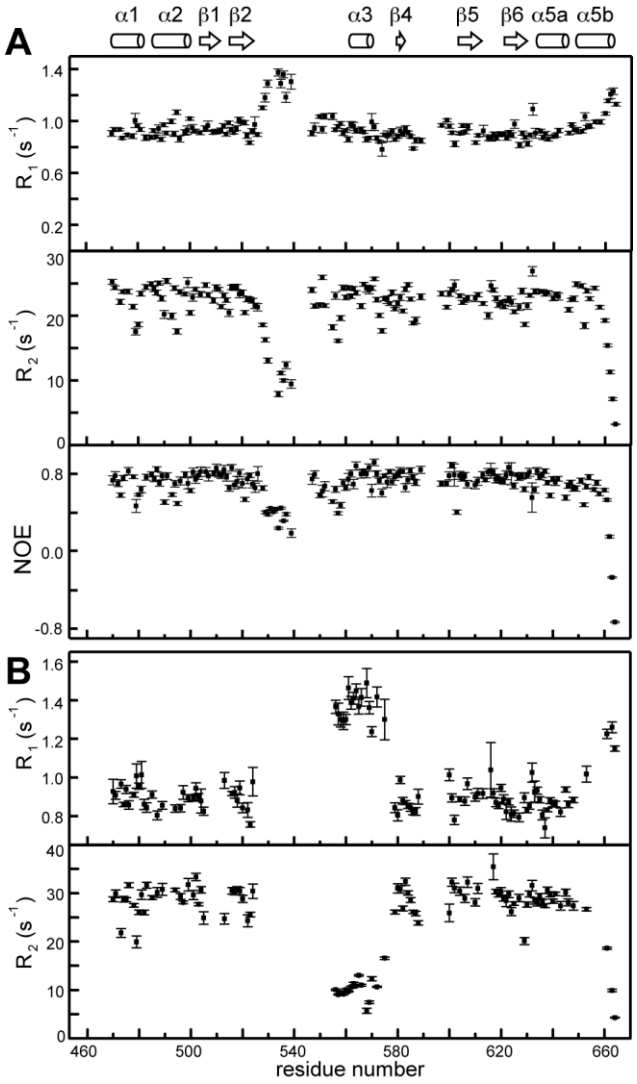

Fig. 3 ^{15}N NMR relaxation data and protein backbone dynamics for individual photostates of NpF2164g3. (A) Light-activated state of NpF2164g3: ^{15}N longitudinal relaxation rate constant, R_1 (top panel), ^{15}N transverse relaxation rate constant, R_2 (middle panel), heteronuclear NOE (bottom panel) plotted as a function of residue number. (B) Dark-state of NpF2164g3: R_1 (top panel) and R_2 (bottom panel) are plotted as a function of residue number.

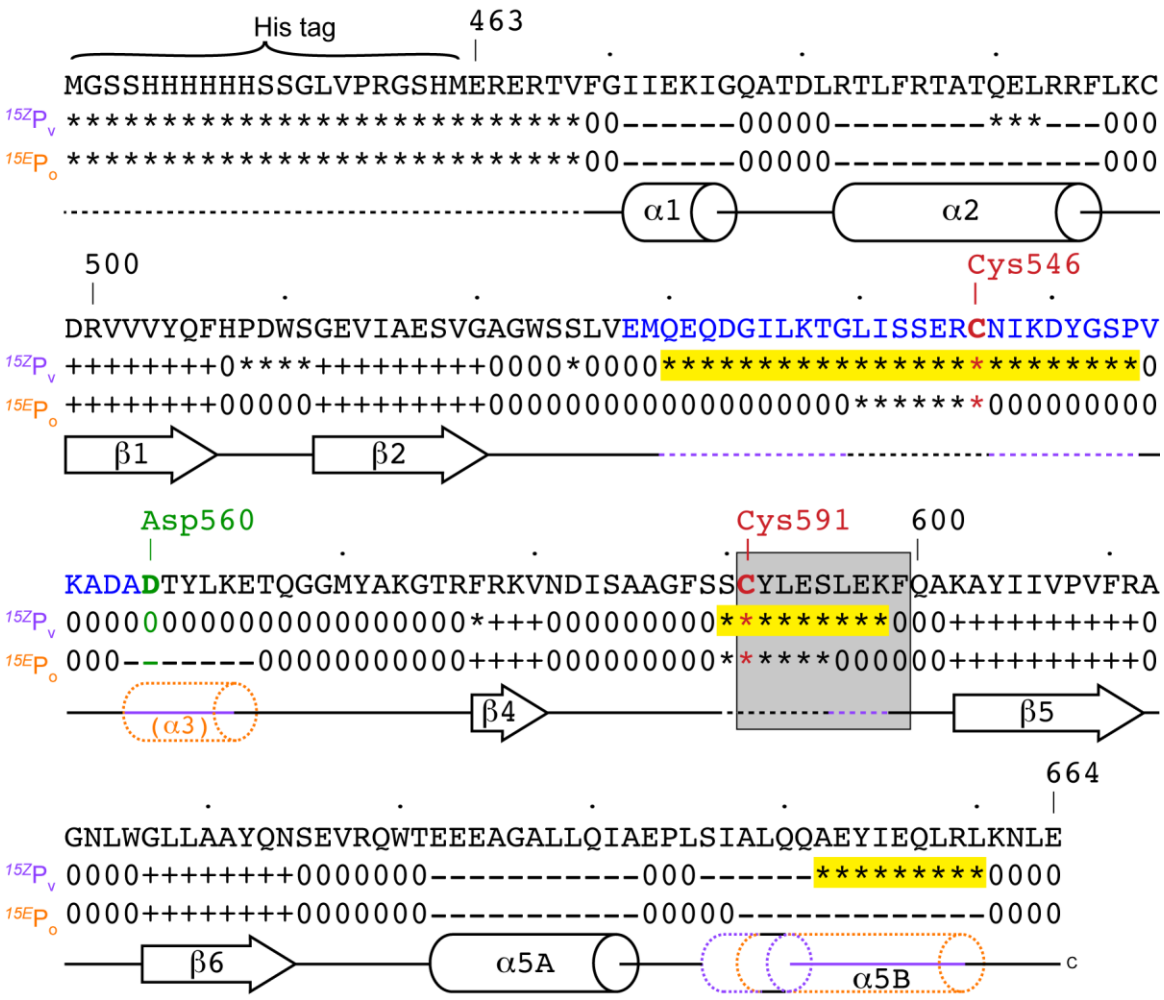

Fig. 4 Secondary structure of NpF2164g3. Secondary structural elements were derived from analysis of chemical shift index[42] and sequential NOE patterns. The chemical shift index sign (+, - or 0) is indicated underneath each residue. Residues in the insert-Cys insertion loop are colored blue. The two cysteine residues (Cys546 and Cys591) linked to the dark-state chromophore are colored red. The Asp-motif residue Asp560 is colored green. Unassigned residues are marked by an asterisk. Residues in the grey box are helical in AnPixJ (Fig. 2). Regions that are exchange broadened in the dark state are highlighted yellow. Regions of variable secondary structure are color-coded.

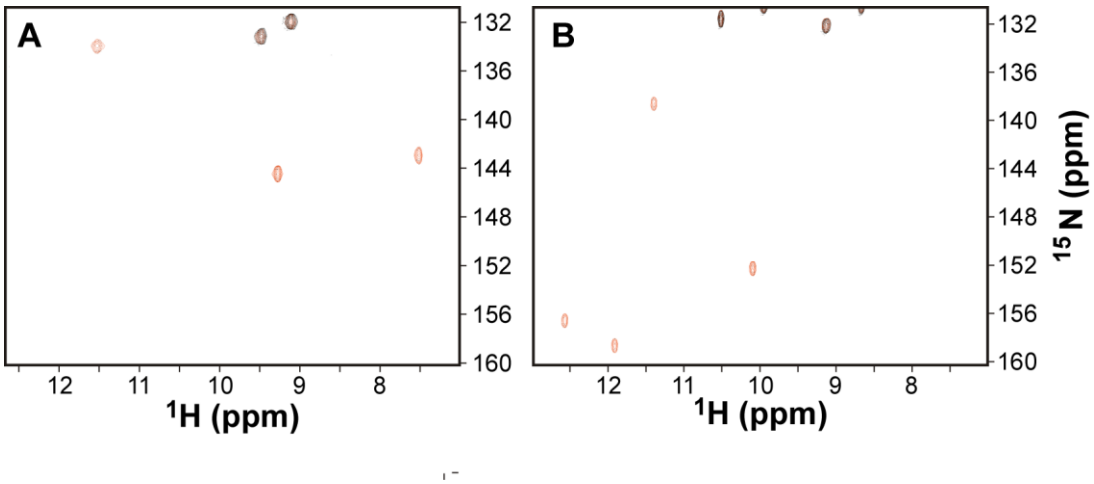

Fig. 5 Two-dimensional ^{15}N-^{1}H HSQC NMR spectra of NpF2164g3 (pyrrole region). (A) NMR spectrum of ^{15}N-labeled NpF2164g3 in the dark-adapted state containing a ^{14}N-labeled bilin chromophore (black) overlaid onto that containing a ^{15}N-labeled bilin chromophore (red). (B) NMR spectrum of light-activated NpF2164g3 containing a ^{14}N-labeled bilin chromophore (black) overlaid onto that containing a ^{15}N-labeled bilin chromophore (red). The non-pyrrole resonances (black at ^{15}N ~ 132 ppm) are due to tryptophan indole side-chain resonances from the ^{15}N-labeled protein. Pyrrole resonances are shown in red.

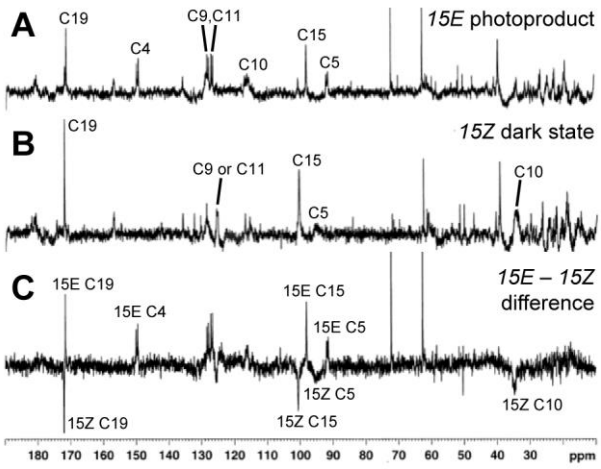

Fig. 6 ^{13}C NMR spectra of NpF2164g3 with attached bilin chromophore containing ^{13}C labeling (at C4, C5, C9, C10, C11, C15, and C19) in the dark-adapted state (A), light-activated state (B), and dark-minus-light difference spectrum (C).

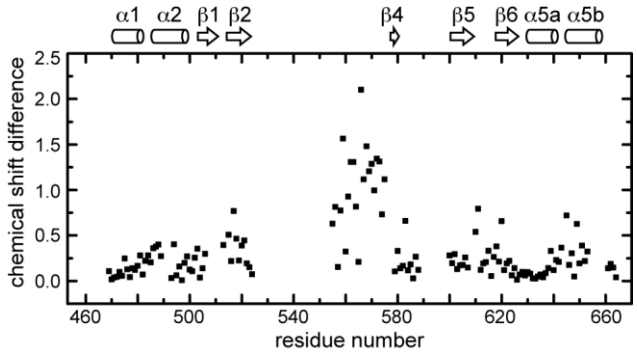

Fig. 7 Light-dependent structural changes in NpF2164g3 plotted as a function of residue number. Chemical shift differences between residues in the dark-state and light-activated states (CSD as defined in the text) are plotted.

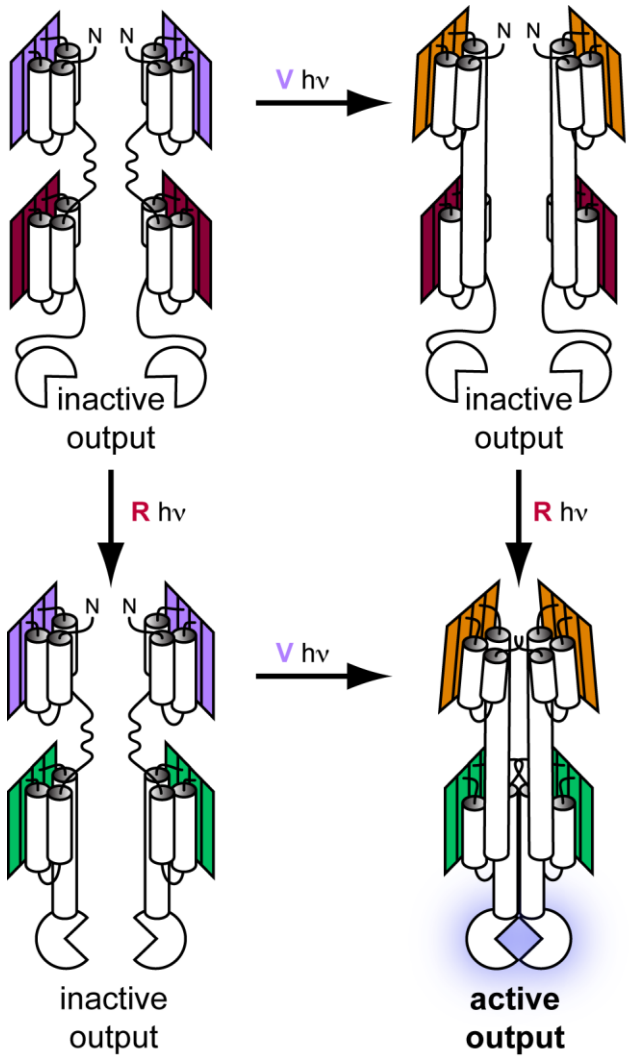

Fig. 8 Hypothetical progressive dimerization model for function of CBCRs in tandem. We consider a simplified CBCR photosensor, comprising an N-terminal violet/orange CBCR, a red/green CBCR, and a C-terminal output domain that requires dimerization for function. When both proteins are in the dark state *(top left)*, the C-terminal α5 helix of each CBCR domain is unstable and the photoreceptor is largely monomeric. Photoconversion of the N-terminal CBCR domain by violet light *(top right)* results in formation of a stable helix connecting the two CBCR domains. Photoconversion of the C-terminal CBCR domain by red light *(bottom left)* results in formation of a stable helix connecting the red/green CBCR domain to the output domain. Photoconversion of both CBCR domains *(bottom right)* provides two stable helices and allows maximal formation of the stable, biologically active output-domain dimer. V, violet; R, red.